LUND UNIVERSITY
Faculty of Medicine

NOVEL BLOCKER OF NFAT ACTIVATION INHIBITS INTERLEUKIN-6 PRODUCTION IN HUMAN MYOMETRIAL ARTERIES AND REDUCES VASCULAR SMOOTH MUSCLE CELL PROLIFERATION

Lisa M. Nilsson[1], Zheng-Wu Sun[1], Jenny Nilsson[1], Ina Nordström[1], Yung-Wu Chen[2], Jeffery D. Molkentin[3], Dag Wide-Swensson[4], Per Hellstrand[1], Marie-Louise Lydrup[5] & Maria F. Gomez[1]

[1]Department of Experimental Medical Science, Lund University, 22184 Lund, Sweden, [2]Global Pharmaceutical Research and Development, Abbott Laboratories, Abbott Park, IL 60064, [3]Department of Pediatrics, Children's Hospital Medical Center, Cincinnati, Ohio, [4]Department of Obstetrics and Gynecology and [5]Department of Surgery, Lund University.

Running head: NFAT in vascular smooth muscle

Address correspondence to: Maria F. Gomez,

Dept. of Experimental Medical Science,

Lund University,

BMC D12, 22184 Lund, Sweden

E-mail: maria.gomez@med.lu.se

Phone: +46-46-2227758 / Fax: +46-46-2224546

Abstract

The calcineurin/NFAT signaling pathway has been found to play a role in regulating growth and differentiation in several cell types. However, the functional significance of NFAT in the vasculature is largely unclear. Here we show that NFATc1, NFATc3 and NFATc4 are expressed in human myometrial arteries. Confocal immunofluorescence and western blot analysis revealed that endothelin-1 efficiently increases NFATc3 nuclear accumulation in native arteries. Endothelin-1 also stimulates NFAT-dependent transcriptional activity, as shown by a luciferase reporter assay. Both the agonist-induced NFAT nuclear accumulation and transcriptional activity were prevented by the calcineurin inhibitor CsA and by the novel NFAT blocker A-285222. Chronic inhibition of NFAT significantly reduced IL-6 production in intact myometrial arteries and inhibited cell proliferation in vascular smooth muscle cells cultured from explants from the same arteries. Further, using small-interfering-RNA-mediated reduction of NFATc3, we show that this isoform is involved in the regulation of cell proliferation. Protein synthesis in intact arteries was investigated using autoradiography of [^{35}S]methionine incorporation in serum-free culture. Inhibition of NFAT signaling did not affect overall protein synthesis or specifically the synthesis rates of major proteins associated with the contractile/cytoskeletal system. An intact contractile phenotype under these conditions was also shown by unchanged force response to depolarization or agonist stimulation. Our results demonstrate NFAT expression and activation in native human vessels and point out A-285222 as a powerful pharmacological blocker of NFAT signaling in the vasculature.

Keywords: Ca^{2+}/calcineurin, endothelin-1, cyclosporin A, contractility, differentiation.

Introduction

Vascular smooth muscle cells (VSMCs) are able to proliferate and assume different phenotypes in response to altered environmental stimuli (26). This is essential for adaptation and survival, e.g. in vasculogenesis and vascular repair after injury, but can also lead to adverse effects and disease, as seen in atherosclerosis, restenosis after angioplasty, and tumor angiogenesis. Among other changes, alterations in Ca^{2+} signaling are frequently observed in disease. However, little is known about how these changes translate into specific genetic programs that may control VSMC growth and differentiation. Ca^{2+}-sensitive transcription factors, such as NFAT (nuclear factor of activated T-cells) are thus attractive candidate mediators of these processes.

The NFAT family consists of four members (NFATc1-c4), which exist as transcriptionally inactive, cytosolic phosphoproteins (27). NFAT nuclear localization is dependent on a dynamic import-export balance between the activity of the Ca^{2+}/calmodulin-dependent phosphatase, calcineurin, and the activity of serine/threonine kinases (4). NFAT was originally described as a transcriptional activator of cytokine and immunoregulatory genes in T-cells (27), but has since also been demonstrated in cells outside the immune system. Loss-of-function mutants have shown that NFAT signaling is crucial for normal skeletal muscle, heart valve and vascular development during embryogenesis (28). Postnatally, this pathway contributes to the regulation of cell growth, differentiation and cell cycle progression in various cell types (18, 36).

In mouse intact arteries and rat VSMCs, we and others have shown that activation of tyrosine kinase and G-protein coupled receptors, which leads to growth stimulation, effectively activates NFAT (9, 24, 37). In cultured VSMCs, NFAT activation was found to increase mi-

gration and proliferation (19, 37), and in a rat carotid artery injury model, blockade of NFAT signaling has been demonstrated to reduce neointima formation (17, 20). Studies in isolated VSMCs have also suggested that NFAT may play a role in smooth muscle differentiation via regulation of smooth muscle-specific markers such as smooth muscle myosin heavy chain (SM-MHC) and α-actin (10, 33). However, the functional significance of NFAT activation in intact as opposed to injured arteries or to isolated VSMCs is still unclear.

Typically, the NFAT pathway has been challenged using calcineurin blockers, such as the immunosuppressant drugs cyclosporin A (CsA), and FK506 (12). Since calcineurin interacts with several substrates apart from NFAT, these drugs are ambiguous tools for mapping the NFAT signaling pathway. In a search for safer immunosuppressive drugs, a series of 3,5-bis(trifluoromethyl)pyrazole (BTP) derivatives were identified as novel NFAT blockers (6, 32). These compounds, such as **A-285222** used in this study, maintain NFAT in a phosphorylated state, blocking its nuclear import and subsequent cytokine gene transcription in immune cells. Inhibition of NFAT is selective, since these compounds did not affect NF-κB or AP-1 activation, or dephosphorylation of other calcineurin substrates such as the type II regulatory subunit of protein kinase A and the transcription factor Elk-1 (32).

The aim of this work was to study NFAT expression and activation properties in an intact human vascular preparation. Further, we wanted to test a novel blocker of the NFAT signaling pathway and investigate the impact of NFAT inhibition on 1) VSMC proliferation, 2) production of interleukin-6 (IL-6), a previously identified NFAT target in cultured VSMCs, 3) expression of proteins associated with the contractile apparatus, and 4) vascular contractility.

Materials and Methods

Human arteries and cells. Intramyometrial resistance arteries from pre-menopausal women undergoing hysterectomy for non-oncologic reasons were used. Arteries (mean lumen diameter 190 μm, 4-6 cell layers) were dissected in Ca^{2+}-free ice-cold physiological saline solution. Vessels were used directly after dissection or after organ culture in DMEM and Ham's F12 (1:1) supplemented with 50 U/ml penicillin and 50 μg/ml streptomycin. This study was approved by the local ethics committee and all women gave their informed consent to participate.

Vascular smooth muscle cells were obtained from explants of human myometrial arteries (hmVSMCs) and of aortas from female NMRI mice (mVSMCs). Cells were cultured in DMEM and Ham's F12 (1:1) supplemented with 15% fetal bovine serum (FBS, Biochrom AG) and used up to passage 7. Human Jurkat cells (ATCC, VA) were cultured in RPMI 1640 (Gibco/BRL, Life Technology Ltd) with 5% FBS, non-essential amino acids (1:100), 1 mM sodium pyruvate and 50 μg/ml gentamycin.

RNA isolation and RT-PCR. RNA isolation (TRIZOL-LS Reagent, Invitrogen Life Technologies) was followed by reverse transcription (Sensiscript RT Kit, Qiagen). cDNA was amplified (HotStarTaq Master Mix Kit, Qiagen) using NFAT isoform-specific primers (Table 1). PCR products were separated by agarose gel electrophoresis and sequenced.

Western blotting. Frozen arteries were placed in Laemmli lysis buffer containing 5% 2-mercaptoethanol and protease inhibitor cocktail (Sigma) at 80-100°C for 15 min. HmVSMCs were collected by scraping, centrifuged and resuspended in Laemmli lysis buffer. Proteins were separated on 12.5 % SDS-PAGE gels, transferred to nitrocellulose membrane (Bio-Rad), probed with primary antibodies overnight and HRP-conjugated secondary anti-

bodies. Labeling was detected by chemiluminescence (Supersignal West Femto, Perbio Science). The primary antibodies used in western blotting were NFATc1 (sc-7294), NFATc3 (sc-8321), NFATc4 (sc-13036), PCNA (sc-56) and cyclin D1 (sc-753, all from Santa Cruz Biotechnology), and GAPDH (Chemicon).

NFATc3 immunofluorescence. HmVSMCs on coverslips and myometrial arteries were treated as specified in the text and fixed in 4% formaldehyde in PBS. Arteries were embedded and cryosectioned (10 μm) after fixation. Immunofluorescence experiments were performed and analyzed as previously described (9, 24). Primary antibody—rabbit anti-NFATc3 (1:250, Santa Cruz Biotechnology) and secondary antibody—Cy5-anti-rabbit IgG (1:500, Jackson ImmunoResearch) were used at excitation-emission wavelengths of 633 and >650 nm, respectively. For identification of smooth muscle cells, arterial sections and hmVSMCs were also stained for SM-α-actin (1:400, Sigma). The fluorescent nucleic acid dye SYTOX Green (1:3000, Molecular Probes) was used for nuclear identification. Cells with deviating nuclear and cellular shapes, which could represent non-smooth muscle cells, were manually excluded from the analysis (2.2% ± 0.5% of all cells counted). Sections and cells were examined at 40X (numerical aperture 1.3) in a Zeiss LSM 5 Pascal laser scanning confocal microscope. For scoring of NFATc3-positive nuclei in arteries, multiple fields for each section were analyzed under blind conditions. A cell was considered positive if co-localization (white) was observed in the nucleus and negative if no co-localization (green only) was observed. For measurement of NFATc3 nuclear accumulation in hmVSMCs, mean fluorescence intensity of nuclear NFATc3 was quantified using the Zeiss LSM 5 analysis software. The same software was used to determine NFATc3 expression in small interfering RNA (siRNA) experiments.

NFATc3 in nuclear extracts. Nuclear extracts were prepared essentially as described before (5). mVSMCs were serum starved for 24 h and treated as specified in the text. Cells were rinsed with ice-cold PBS, harvested by trypsination, centrifuged at 850 x g (4°C, 3 min) and resuspended in 80 µL of lysis buffer containing (in mmol/L) Tris (pH 7.3) 10, KCl 10, and $MgCl_2$ 1.5, and 0.4% NP-40. 2-Mercaptoethanol (5 mmol/L) and protease inhibitor cocktail (Sigma) were added to all buffers. After incubation at 4°C for 2 min, nuclei were collected by centrifugation (1 min, 9000 x g). Pellets were washed once in 500 µL of 20 mmol/L KCl buffer, containing (in mmol/L) Tris (pH 7.3) 20, KCl 20, $MgCl_2$ 1.5, EDTA 0.2 and 21.75% glycerol. Isolated nuclei were resuspended in 15 µL of 20 mmol/L KCl buffer and 60 µL of 600 mmol/L KCl buffer containing (in mmol/L) Tris (pH 7.3) 20, KCl 600, $MgCl_2$ 1.5, EDTA 0.2 and 21.75% glycerol. Nuclear proteins were extracted by incubation on ice for 30 min. After centrifugation at 9000 x g (4°C, 15 min), the supernatant containing nuclear proteins was transferred to a precooled microcentrifuge tube and used for western blotting. Purity of nuclear fractions was demonstrated by lack of immunoreactivity for the cytosolic marker GAPDH. The nuclear marker PCNA was used for equal loading of nuclear fractions.

Luciferase Reporter Assay. Phenotypically normal, female NFAT-luc transgenic mice were used (35). These mice express nine copies of an NFAT binding site from the interleukin-4 promoter, positioned 5' to a minimal promoter from the α-myosin heavy chain gene (-164 to +16) and inserted upstream of a luciferase reporter gene. Animals were euthanized by peritoneal injection of pentobarbital solution (200 mg/kg) as approved by the local animal ethics committee. Aortas were dissected, treated as specified in the text and homogenized in lysis buffer: 100 mM KPO_4 (pH 7.8), 0.5% NP-40 and 1 mM DTT. An aliquot of supernatant, obtained by centrifugation at 13200 x *g* for 15 min, was added to luciferase sub-

strate reagent: 100 mM Tris-HCl (pH 7.8), 10 mM MgAcetate, 1 mM EDTA, 1.4 mM luciferin (Promega) and 18.3 mM ATP. Optical density was measured (VICTOR 3 multilabel counter, PerkinElmer), normalized to protein concentration as determined by Bradford assay (BioRad) and expressed as relative luciferase units.

Proliferation measurements. HmVSMCs grown on coverslips were treated as specified in the text and fixed in ice-cold methanol. Immunofluorescence experiments were performed as described above, using a monoclonal antibody against PCNA (proliferating cell nuclear antigen, PC10, Santa Cruz Biotechnology) and a Cy5-anti-mouse secondary antibody (Jackson ImmunoResearch). Nuclear regions and individual cells were identified using SYTOX Green. Using the Zeiss LSM 5 analysis software, PCNA expression was measured after background subtraction by calculating the relative number of pixels positive for PCNA in the nuclei. For PCNA experiments, 5-10 images per coverslip obtained at 40X, and at least 2 coverslips per treatment were examined per experiment. Cell number was counted manually from 3-5 images per coverslip obtained at 10X, and at least 4 coverslips per treatment and experiment. All experiments were conducted under blind conditions. Cell proliferation was also assessed by measuring the expression cyclin D1 in western blot experiments.

Small interfering RNA transfection. HmVSMCs were transfected with NFATc3 ON-TARGET plus SMART pool siRNA (Dharmacon) or siCONTROL Non-Targeting siRNA pool (Dharmacon), complexed with Lipofectamine 2000 (Invitrogen) in antibiotics free medium, according to the manufacturer's instructions. SMART pool reagents combine four SMART selection-designed siRNAs into a single pool. SiRNAs were used at a final concentration of 82.5-100 nM. After 6 h, RNA/lipid complexes were removed, and cells were incubated for another 72-120 h in culture medium supplemented with 1.5% FBS. NFATc3 ex-

pression in siRNA treated hmVSMCs was determined using western blotting and confocal immunofluorescence. Proliferation was assessed by blotting for cyclin D1. The transfection efficiency was determined by measuring uptake of a fluorescently labeled siRNA (siGLO Lamin A/C siRNA, 82.5 nM, Dharmacon). 24 h after transfection start, approximately 90% of the cells were positive for siGLO Lamin A/C siRNA.

IL-6 ELISA. Intact arteries were cultured for 4 days with or without A-285222 or cyclosporin A (CsA, Sigma). The amounts of interleukin-6 (IL-6) released into the culture medium were assayed using ELISA human IL-6 DuoSet Kit (R&D Systems, Abingdon UK). Absorbance was measured at 450 nm and the lower limit of detection was 10 pg/mL. IL-6 concentrations were normalized to total protein content determined by the Bradford assay (Bio-Rad), and all experiments were conducted in duplicate.

Protein separation and autoradiography. Intact arteries were cultured for 4 days with or without A-285222 or cyclosporin A. After culture, arteries were frozen, pulverized in liquid N_2, and proteins extracted with SDS-containing buffer. Total protein concentration was determined using RediPlate EZQ Protein Quantitation kit (Molecular Probes). Proteins were separated by electrophoresis on 12.5% SDS-polyacrylamide gels, with a load of 10 μg protein in each lane and subsequent Coomassie blue staining. Protein synthesis was measured by autoradiography as described earlier (2). Briefly, intact arteries were kept in organ culture for 72 h and then exposed to [^{35}S]methionine in a low-methionine medium for another 24 h. The tissue was frozen, proteins separated as above, whereafter gels were dried and autoradiographed. Gels and autoradiographs were scanned and bands corresponding to actin and SM22α were analysed using gel analysis software (Quantity-One, BioRad). Proteins were identified by Western blotting using specific antibodies (2).

Contractility measurements. Fresh and cultured myometrial arteries were mounted for isometrical force measurements on 40-μm stainless steel wires on a tension myograph (610M, Danish Myo Technology A/S, Aarhus, Denmark) as previously described (7). For all force experiments using cultured arteries, segments of fresh arteries were divided in halves and cultured in parallel with or without A-285222 or CsA (0.1 and 1.0 μmol/L, respectively), for paired comparisons. Arteries were stretched to a passive tension of 2 mN, which was previously determined as optimal pre-load. Preparations were allowed to equilibrate in PSS containing 2.5 mmol/L Ca^{2+} at 37°C for at least 30 min before stimulation. High K^+ solution (HK, 60 mmol/L) and 10 nmol/L Et-1 were used since they yielded maximal force in dose-response experiments (not shown). HK was prepared by replacing NaCl with KCl, and applied as consecutive 10 min stimulation until stable responses were obtained. Due to the irreversible nature of Et-1 responses, only single doses of Et-1 were applied at the end of the stimulation protocol. Wall tension is expressed as recorded force divided by twice the vessel length, normalized to the number of cell layers. For determination of the number of cell layers, arteries were routinely fixed after force measurements, embedded, frozen and cryosectioned, followed by staining with the fluorescent nuclear dye SYTOX Green (1:3000).

Statistical analysis. Results are expressed as means ± S.E.M (n = patients or mice). Statistical significance was determined using Student's t-test or one-way ANOVA followed by Bonferroni or Tukey-Kramer tests, for single and multiple comparisons, respectively. *P<0.05, **P<0.01 and ***P<0.001.

Results

NFAT isoform expression in human vascular smooth muscle. Using RT-PCR analysis, NFATc1, NFATc3 and NFATc4 were successfully amplified in intact human myometrial arteries (Fig.1*A*). In contrast to what has been described in vascular smooth muscle from mouse (9, 29), substantial levels of NFATc1 were detected in these vessels. No NFATc2 expression was found in native non-stimulated vessels (Fig. 1*A*) using primer pairs that efficiently amplify NFATc2 in Jurkat cells ((27), Fig. 1*B*). When experiments were repeated in hmVSMCs, the same pattern of NFAT expression was found (Fig 1*C*). Surprisingly, NFATc2 was detected if myometrial vessels were cultured for 4 days, suggesting that expression of this isoform might be induced or enhanced under certain conditions (Fig. 1*D*). Western analysis showed discrete bands for NFATc1, NFATc3 and NFATc4 proteins in myometrial arteries, corresponding to previously reported sizes (Fig. 1*E*).

Endothelin-1 (Et-1)-induced NFATc3 nuclear accumulation and NFAT-dependent transcriptional activity. Et-1 is a potent vasoconstrictor agonist that activates G-protein coupled receptors and increases intracellular Ca^{2+} and has previously been shown to effectively increase NFATc3 nuclear accumulation in mouse cerebral arteries (9). Here we find that treatment with Et-1 increases NFATc3 nuclear accumulation in hmVSMCs as evidenced by colocalization of NFATc3 with the nucleic acid dye SYTOX Green. This occurs in a time-dependent manner, showing a transient maximum level at 30 min and returning to control values at 60 min (Fig. 2*A* and *B*). VSMCs represent 98% of the cells present in the arterial explants and stain positive for SM-α-actin (Fig. 2*C*). Agonist-induced NFATc3 nuclear accumulation was confirmed by western blot analysis of nuclear fractions. As shown in Fig. 2*D*, 30 min stimulation with Et-1 results in increased nuclear NFATc3 levels.

In intact myometrial arteries, incubation with Et-1 for 30 min significantly increased the number of NFATc3-positive nuclei from 16% to 66% (Fig. 3*A*). In order to test whether agonist stimulation and the concomitant NFATc3 nuclear accumulation leads to enhanced NFAT-dependent transcriptional activity, we used arteries from NFAT-luciferase reporter transgenic mice. Indeed, treatment of mouse aorta with Et-1 for 30 min resulted in a significant increase in NFAT-dependent luciferase activity compared to control levels in non-stimulated arteries (Fig. 3*C*).

A-285222 blocks agonist-induced NFAT activation. Incubation of intact myometrial arteries with the NFAT-blocker A-285222 prior to (30 min) and concurrent with 30 min Et-1 stimulation prevented agonist-induced NFATc3 nuclear accumulation, yielding levels not different from non-stimulated control vessels (Fig.3*A* and *B*). Consistent with studies in human T-cells (6), the effect of A-285222 was significant at 0.1 μmol/L. A-285222 also prevented the increased NFATc3 accumulation in nuclear fractions from VSMCs (Fig. 2*C*). Further, A-285222 effectively blocked the enhanced NFAT-dependent transcriptional activity induced by Et-1 in aortas from NFAT-luciferase reporter mice (Fig. 3*C*). Inhibition of calcineurin activity with CsA also blocked agonist-induced NFAT activation, as shown in immunofluorescence and luciferase experiments (Fig. 3*B* and *C*). Moreover, inhibition of voltage-dependent Ca^{2+}-channels (VDCC) with verapamil abolished Et-1-induced NFATc3 nuclear accumulation (Fig. 3*B*). In agreement with previous studies (8, 9, 29) 30 min depolarization with 60 mmol/L K^+ solution alone failed to induce NFATc3 nuclear accumulation (data not shown, n=3), suggesting that extracellular Ca^{2+} inflow is necessary but not sufficient for NFATc3 activation.

Proliferation of hmVSMCs is inhibited by NFAT blockade. NFAT activation has previously been shown to enhance proliferation in murine VSMCs (20, 37, 38). We therefore investigated the effect of the NFAT blocker A-285222 on VSMC proliferation. For this, we exposed highly proliferating hmVSMCs (cultured in 15% FBS) to A-285222 and measured the expression of the S-phase marker PCNA and changes in total cell number. As shown in Fig. 4*A* and *B*, 48 h culture of hmVSMCs with 1 μmol/L A-285222 resulted in a significant reduction of PCNA expression (69% of control) and a corresponding decrease in total cell number (76% of control). We also evaluated the effect of NFAT inhibition on Et-1-driven cell proliferation using western blot analysis of the G_1-phase marker cyclin D1. As seen in Fig. 4*C*, 24 h culture of hmVSMCs with 1 μmol/L A-285222 resulted in a 40% reduction of cyclin D1 expression. Culture with 1 μmol/L CsA had no significant effect on PCNA expression or total cell number (Fig. 4*A* and *B*), whereas higher doses of CsA (3 and 10 μmol/L) reduced cell number (93% and 80% of control, Fig. 4*D*) but to a lesser extent than corresponding doses of A-285222. For comparison, PCNA expression and cell number were assessed after 48 h of serum starvation. As expected, proliferation was significantly reduced, which is shown by a reduction of PCNA expression to 38% of control and a decrease in the total number of cells to 59% (Fig. 4*A* and *B*). The dose-response relationship of A-285222 on hmVSMC proliferation revealed an EC50 value of 1.07 μmol/L (Fig. 4*D*).

NFATc3 is involved in the regulation of VSMC proliferation. To substantiate the role of NFATc3 in VSMC proliferation, an siRNA approach was used to down regulate this specific isoform. Using confocal immunofluorescence microscopy, we show that the expression of NFATc3 in hmVSMCs was depressed to 77% of control 72 h after transfection with siRNA specific for NFATc3 (Fig. 5*A*). Using western blot analysis, NFATc3 expression was found to be 66% of control 120 h after transfection in hmVSMCs (Fig. 5*B*). In these cells, a

concomitant reduction of cyclin D1 levels was observed (Fig. 5B), demonstrating the involvement of NFATc3 in the regulation of VSMC proliferation.

Chronic inhibition of NFAT prevents IL-6 production in intact arteries. Earlier studies have shown in rat thoracic VSMCs that receptor tyrosine kinase and G-protein coupled receptor agonists induce IL-6 expression in an NFAT-dependent manner (1, 19). To study if NFAT is involved in the regulation of IL-6 expression in native arteries, we cultured intact myometrial arteries for 4 days in the presence or absence of A-285222 or CsA and measured the amount of IL-6 release to the culture medium. As shown in Fig. 6, IL-6 production during the culture period was significantly reduced upon inhibition of NFAT signaling with both blockers. The same level of IL-6 inhibition was obtained with 0.1 and 1.0 μmol/L A-285222.

Synthesis of contractile proteins is not affected by NFAT inhibition during culture of intact arteries. Protein contents were studied after culture of non-stimulated myometrial arteries for 4 days in the presence or absence of A-285222 or CsA. Proteins separated on SDS gels were visualized by Coomassie blue staining and bands corresponding to actin and SM22α were evaluated. As shown in Fig. 7*A*, no clear difference in the distribution pattern of proteins between control and treated vessels was observed. Summarized data from Coomassie-gels show no significant changes on the total contents of actin and SM22 α (Fig. 7*B*). Since the culture time used here (4 days) may not be sufficient to cause measurable changes in the relative contents of these contractile proteins, protein synthesis rates upon NFAT signaling inhibition were studied from autoradiographs. A small but not statistically significant decrease in total and individual (actin and SM22 α) protein synthesis was ob-

served after treatment with CsA, whereas no effect was found with A-285222 (Fig. 7*C* and *D*).

Chronic inhibition of NFAT signaling has no effect on vascular contractility. To study whether long-term depression of NFAT signaling had any impact on contractile ability, we divided myometrial arteries in equal segments and cultured them in parallel for 4 days in the presence or absence of A-285222 or CsA. After the culture period, the vessels were mounted isometrically and contracted with 60 mmol/L KCl (HK) and then with Et-1. Neither depolarization- nor agonist-induced contractions were affected by 4-day treatment with A-285222 or CsA when compared with controls (Fig.8*A*-*D*). We also tested acute doses of A-285222 (0.1, 1 and 10 μM) on basal force, HK- and Et-1-induced responses and found no effects (data not shown). The number of cell layers after 4 day treatment with A-285222 or CsA was not affected when compared with control untreated vessels (4.0 ± 0.3 vs. 4.9 ± 0.4 for A-285222; 5.6 ± 0.2 vs. 5.7 ± 0.4 for CsA).

Discussion

Previous work has demonstrated NFATc3 to be the predominant isoform expressed in intact smooth muscle from mouse, whereas smaller amounts of NFATc4 were detected (9, 29). In cultured smooth muscle cells from human and rat aorta, all isoforms have been detected (30, 33, 37). In human myometrial vessels and in hmVSMCs, we not only found NFATc3 and NFATc4, but also NFATc1, suggesting different patterns of expression depending on species and/or vascular bed. Interestingly, NFATc2 could only be detected in cultured arteries, indicating that this isoform might be induced under certain conditions. This observation hints at the untested possibility that changes in NFAT isoform expression, by virtue of a differential effect on target genes, might have implications for smooth muscle adaptation to environmental challenge.

As previously described, G-protein and tyrosine kinase coupled receptor stimulation effectively induces NFATc3 nuclear accumulation in VSMCs and intact murine arteries (1, 9, 19, 24). Here we show that Et-1, which is a potent vasoconstrictor agonist in the uterine circulation (15), significantly increases NFATc3 nuclear accumulation in intact human arteries. In agreement with previous studies (8, 9, 29), Ca^{2+}-influx and calcineurin activation are clearly necessary for Et-1-induced NFATc3 response, as evidenced by the ability of the VDCC blocker verapamil and CsA to prevent nuclear accumulation of NFATc3. Further, the observed time-course of NFAT activation suggests preserved kinetics among different species and types of smooth muscle.

In this study, the effects of A-285222, previously shown to be an effective NFAT blocker in T-cells, were evaluated in smooth muscle. Agonist stimulation not only leads to increased NFATc3 nuclear accumulation, but also to increased NFAT-dependent transcrip-

tional activity in intact arteries, as shown in the luciferase experiments. A-285222, as well as the calcineurin inhibitor CsA clearly blocked Et-1-induced NFATc3 nuclear accumulation and NFAT-dependent transcriptional activity. Furthermore, A-285222 and CsA both lowered IL-6 production in human arteries, demonstrating a functional correlate to the inhibition of NFATc3 nuclear accumulation.

A role for NFAT in VSMC proliferation has been proposed from experiments using thrombin- and PDGF-induced cell growth in VSMCs from rat aorta (37). Growth, as determined by [^{3}H]thymidine incorporation and increase in cell number, was inhibited by CsA (10 μmol/L) or by forced expression of the peptide VIVIT, which competes with NFAT for calcineurin binding (37). Here we show that NFAT inhibition with the novel compound A-285222 significantly reduces FBS- and Et-1-induced proliferation in human VSMCs. Further, using an siRNA approach, we provide for the first time direct evidence for the involvement of NFATc3 in the regulation of VSMC proliferation. Interestingly, Bushdid et al (3) provided indirect evidence for a proliferative role of this isoform in vascular smooth muscle during development. These authors found a reduced number of α-actin positive SMCs in the dorsal aortas of *nfatc3*$^{-/-}$*nfatc4*$^{-/-}$ mice when compared to aortas of *nfatc3*$^{+/+}$*nfatc4*$^{-/-}$ mice.

In our study, only 10 μmol/L CsA significantly reduced the total number of VSMCs in culture, whereas 1 μmol/L CsA had no effect on cell proliferation, despite the fact that it acutely blocked NFATc3 nuclear accumulation and NFAT-dependent transcriptional activity. One possible interpretation to this discrepancy would be that there are other processes evoked by CsA which are independent of NFAT signaling. At least two well-established downstream targets of calcineurin, PKA and Elk-1, have been shown to regulate VSMC proliferation (13, 34). In human pulmonary artery VSMCs, Medina & Wolf demonstrated a

paracrine/autocrine release of Et-1 upon CsA treatment, leading to increased VSMC proliferation (21). A potential CsA-induced release of Et-1, or the activation of alternative downstream targets may counteract any anti-proliferative effect achieved via inhibition of the calcineurin-NFAT signaling pathway. It is therefore not unlikely that calcineurin inhibition with CsA, as opposed to NFAT inhibition with A-285222, would result in less clear effects on VSMC proliferation or cell number. Conflicting results regarding the effects of calcineurin inhibition with CsA on VSMC proliferation have been previously reported, ranging between inhibition, no effects and stimulation of cell proliferation (14, 21, 31). Differences have been attributed to variation in dosage, exposure time, and differences among species or tissue origin of the SMCs. Further, the anti-proliferative effects of CsA in many of these studies are apparent in the range of concentrations that are cytotoxic for the cells (11, 21). The effective inhibition of proliferation by 1 μmol/L A-285222 points to this compound as an interesting alternative to CsA.

Previous work in VSMCs has shown that NFAT participates as a cofactor in NF-κB dependent activation of IL-6 gene expression (1, 19). In these studies, CsA and expression of a trans-dominant NFAT inhibitor prevented agonist-induced IL-6 increase, whereas overexpression of NFAT markedly augmented IL-6 mRNA. Here we show that inhibition of NFAT activity by A-285222 and CsA effectively lowered IL-6 production during organ culture of intact vascular preparations. The levels of this proinflammatory cytokine are usually elevated after vessel injury, and anti-inflammatory strategies that reduce IL-6 levels have proven effective in reducing neointima formation (23). VSMC migration and proliferation are key features of neointima formation in response to intimal lesions. A potential role for NFAT in the regulation of neointima formation following balloon injury in rat carotid artery has already been proposed from studies showing reduced neointima upon exposure to CsA or injec-

tion of adenovirus coding for a competitive peptide inhibitor of the calcineurin/NFAT pathway (20). The novel cell permeable blocker of the NFAT signaling pathway in vascular smooth muscle introduced in the present study may provide an attractive alternative approach to attenuate the response to vascular injury.

Long-term NFAT inhibition with A-285222 or CsA had no significant effect on depolarization- and agonist-induced force development in intact myometrial resistance arteries. In combination with the virtually unchanged pattern of protein contents and synthesis rates, this suggests that inhibition of NFAT basal activity does not lead to VSMC dedifferentiation in native arteries. The organ culture experiments described here were done in serum-free medium, which is known to preserve vascular contractility (16, 40). This condition is expected to give a lower rate of protein synthesis than that observed upon growth-stimulation; however, studies in cultured cells demonstrated an effect of NFAT inhibition on the expression of smooth muscle genes only under growth-arrested conditions (33). The expression of most smooth muscle-specific genes is regulated by serum response factor (SRF) binding to multiple copies of a specific element (CArG box) present in their promotor regions (22). An NFAT-binding element was identified in the smooth muscle α-actin gene by Gonzalez Bosc et al (10), who also demonstrated that NFAT inhibition affects α-actin gene expression in VSMCs. To date, interaction between NFAT and SRF at regulatory sites of other smooth muscle-specific genes has not been demonstrated. A different mechanism involving the interaction of NFAT with a cofactor (GATA-6) has been described to regulate the expression of the SRF-regulated SM-MHC gene (33). Our results suggest that in an intact vascular environment, the expression of smooth muscle specific genes is unlikely to be regulated in an NFAT-sensitive manner. In particular, the synthesis of SM22α, which is a major protein band and a sensitive smooth muscle marker (25, 39), is unaffected. Nevertheless, these re-

sults do not exclude effects of NFAT on the synthesis of less abundant proteins of possibly profound functional importance. Indeed, the effect of NFAT inhibition on IL-6 production under these same non-stimulated conditions demonstrates that NFAT activity is present and influences gene expression. A further possibility is that effects of NFAT on gene expression are mediated indirectly via autocrine release of inflammatory mediators such as IL-6.

This study indicates that whereas NFAT inhibition decreases proliferation of growth-stimulated VSMCs, it has only minor effects on the intact vascular wall, where smooth muscle cells are kept in a quiescent contractile phenotype under the influence of the intact tissue environment. These results suggest NFAT as an interesting target for preventing and treating smooth muscle cell proliferation in vascular disease. The introduction of a novel NFAT inhibitor, A-285222, offers new possibilities to overcome adverse effects of previously used calcineurin inhibitors.

Acknowledgements

We thank Dr. Päivi Kannisto for providing biopsies. This work was supported by Wenner-Gren, Swedish Heart and Lung, Söderberg, Crafoord, Bergvall, Wiberg and Zoéga Foundations, the Royal Physiographic Society, the Swedish Research Council (#71X-28) and the Vascular Wall Program at the Medical Faculty in Lund.

References

1. **Abbott KL, Loss JR, 2nd, Robida AM, and Murphy TJ.** Evidence that Galpha(q)-coupled receptor-induced interleukin-6 mRNA in vascular smooth muscle cells involves the nuclear factor of activated T cells. *Mol Pharmacol* 58: 946-953, 2000.

2. **Albinsson S, Nordstrom I, and Hellstrand P.** Stretch of the vascular wall induces smooth muscle differentiation by promoting actin polymerization. *J Biol Chem* 279: 34849-34855, 2004.

3. **Bushdid PB, Osinska H, Waclaw RR, Molkentin JD, and Yutzey KE.** NFATc3 and NFATc4 are required for cardiac development and mitochondrial function. *Circ Res* 92: 1305-1313, 2003.

4. **Crabtree GR.** Generic signals and specific outcomes: signaling through Ca2+, calcineurin, and NF-AT. *Cell* 96: 611-614, 1999.

5. **Dichtl W, Nilsson L, Goncalves I, Ares MPS, Banfi C, Calara F, Hamsten A, Eriksson P, and Nilsson J.** Very Low-Density Lipoprotein Activates Nuclear Factor-{kappa}B in Endothelial Cells. *Circ Res* 84: 1085-1094, 1999.

6. **Djuric SW, BaMaung NY, Basha A, Liu H, Luly JR, Madar DJ, Sciotti RJ, Tu NP, Wagenaar FL, Wiedeman PE, Zhou X, Ballaron S, Bauch J, Chen YW, Chiou XG, Fey T, Gauvin D, Gubbins E, Hsieh GC, Marsh KC, Mollison KW, Pong M, Shaughnessy TK, Sheets MP, Smith M, Trevillyan JM, Warrior U, Wegner CD, and Carter GW.** 3,5-Bis(trifluoromethyl)pyrazoles: a novel class of NFAT transcription factor regulator. *J Med Chem* 43: 2975-2981, 2000.

7. **Dreja K, Bergdahl A, and Hellstrand P.** Increased store-operated Ca2+ entry into contractile vascular smooth muscle following organ culture. *J Vasc Res* 38: 324-331, 2001.

8. **Gomez MF, Bosc LV, Stevenson AS, Wilkerson MK, Hill-Eubanks DC, and Nelson MT.** Constitutively elevated nuclear export activity opposes Ca2+-dependent NFATc3 nuclear accumulation in vascular smooth muscle: role of JNK2 and Crm-1. *J Biol Chem* 278: 46847-46853, 2003.

9. **Gomez MF, Stevenson AS, Bonev AD, Hill-Eubanks DC, and Nelson MT.** Opposing actions of inositol 1,4,5-trisphosphate and ryanodine receptors on nuclear factor of activated T-cells regulation in smooth muscle. *J Biol Chem* 277: 37756-37764, 2002.

10. **Gonzalez Bosc LV, Layne JJ, Nelson MT, and Hill-Eubanks DC.** Nuclear factor of activated T cells and serum response factor cooperatively regulate the activity of an alpha-actin intronic enhancer. *J Biol Chem* 280: 26113-26120, 2005.

11. **Hafizi S, Mordi VN, Andersson KM, Chester AH, and Yacoub MH.** Differential effects of rapamycin, cyclosporine A, and FK506 on human coronary artery smooth muscle cell proliferation and signalling. *Vascul Pharmacol* 41: 167-176, 2004.

12. **Ho S, Clipstone N, Timmermann L, Northrop J, Graef I, Fiorentino D, Nourse J, and Crabtree GR.** The mechanism of action of cyclosporin A and FK506. *Clin Immunol Immunopathol* 80: S40-45, 1996.

13. **Hogarth DK, Sandbo N, Taurin S, Kolenko V, Miano JM, and Dulin NO.** Dual role of PKA in phenotypic modulation of vascular smooth muscle cells by extracellular ATP. *Am J Physiol Cell Physiol* 287: C449-456, 2004.

14. **Hu SJ, Fernandez R, and Jones JW, Jr.** Cyclosporine A stimulates proliferation of vascular smooth muscle cells and enhances monocyte adhesion to vascular smooth muscle cells. *Transplant Proc* 31: 663-665, 1999.

15. **Kublickiene KR, Wolff K, Kublickas M, Lindblom B, Lunell NO, and Nisell H.** Effects of isradipine on endothelin-induced constriction of myometrial arteries in normotensive pregnant women. *Am J Hypertens* 7: 50S-55S, 1994.

16. **Lindqvist A, Nordstrom I, Malmqvist U, Nordenfelt P, and Hellstrand P.** Long-term effects of Ca(2+) on structure and contractility of vascular smooth muscle. *Am J Physiol* 277: C64-73, 1999.

17. **Lipskaia L, del Monte F, Capiod T, Yacoubi S, Hadri L, Hours M, Hajjar RJ, and Lompre AM.** Sarco/endoplasmic reticulum Ca2+-ATPase gene transfer reduces vascular smooth muscle cell proliferation and neointima formation in the rat. *Circ Res* 97: 488-495, 2005.

18. **Lipskaia L and Lompre AM.** Alteration in temporal kinetics of Ca2+ signaling and control of growth and proliferation. *Biol Cell* 96: 55-68, 2004.

19. **Liu Z, Dronadula N, and Rao GN.** A novel role for nuclear factor of activated T cells in receptor tyrosine kinase and G protein-coupled receptor agonist-induced vascular smooth muscle cell motility. *J Biol Chem*, 2004.

20. **Liu Z, Zhang C, Dronadula N, Li Q, and Rao GN.** Blockade of nuclear factor of activated T cells activation signaling suppresses balloon injury-induced neointima formation in a rat carotid artery model. *J Biol Chem* 280: 14700-14708, 2005.

21. **Medina J and Wolf A.** Strategies to antagonise the cyclosporine A-induced proliferation of human pulmonary artery smooth muscle cells: anti-endothelin-1 antibodies, verapamil, and octreotide. *Biochem Pharmacol* 59: 1459-1466, 2000.

22. **Miano JM.** Serum response factor: toggling between disparate programs of gene expression. *J Mol Cell Cardiol* 35: 577-593, 2003.

23. **Nagasaki K, Matsumoto K, Kaneda M, Shintani T, Shibutani S, Murayama T, Wakabayashi G, Shimazu M, Mukai M, and Kitajima M.** Effects of preinjury administration of corticosteroids on pseudointimal hyperplasia and cytokine response in a rat model of balloon aortic injury. *World J Surg* 28: 910-916, 2004.

24. **Nilsson J, Nilsson LM, Chen YW, Molkentin JD, Erlinge D, and Gomez MF.** High Glucose Activates Nuclear Factor of Activated T Cells in Native Vascular Smooth Muscle. *Arterioscler Thromb Vasc Biol* 26: 794-800, 2006.

25. **Owens GK.** Regulation of differentiation of vascular smooth muscle cells. *Physiol Rev* 75: 487-517, 1995.

26. **Owens GK, Kumar MS, and Wamhoff BR.** Molecular regulation of vascular smooth muscle cell differentiation in development and disease. *Physiol Rev* 84: 767-801, 2004.

27. **Rao A, Luo C, and Hogan PG.** Transcription factors of the NFAT family: regulation and function. *Annu Rev Immunol* 15: 707-747, 1997.

28. **Schulz RA and Yutzey KE.** Calcineurin signaling and NFAT activation in cardio-vascular and skeletal muscle development. *Dev Biol* 266: 1-16, 2004.

29. **Stevenson AS, Gomez MF, Hill-Eubanks DC, and Nelson MT.** NFAT4 movement in native smooth muscle. A role for differential Ca(2+) signaling. *J Biol Chem* 276: 15018-15024, 2001.

30. **Suzuki E, Nishimatsu H, Satonaka H, Walsh K, Goto A, Omata M, Fujita T, Nagai R, and Hirata Y.** Angiotensin II induces myocyte enhancer factor 2- and calcineurin/nuclear factor of activated T cell-dependent transcriptional activation in vascular myocytes. *Circ Res* 90: 1004-1011, 2002.

31. **Tavares P, Martinez-Salgado C, Eleno N, Teixeira F, and Lopez Novoa JM.** Effect of cyclosporin A on rat smooth-muscle cell proliferation. *J Cardiovasc Pharmacol* 31: 46-49, 1998.

32. **Trevillyan JM, Chiou XG, Chen YW, Ballaron SJ, Sheets MP, Smith ML, Wiedeman PE, Warrior U, Wilkins J, Gubbins EJ, Gagne GD, Fagerland J, Carter GW, Luly JR, Mollison KW, and Djuric SW.** Potent inhibition of NFAT activation and T

cell cytokine production by novel low molecular weight pyrazole compounds. *J Biol Chem* 276: 48118-48126, 2001.

33. **Wada H, Hasegawa K, Morimoto T, Kakita T, Yanazume T, Abe M, and Sasayama S.** Calcineurin-GATA-6 pathway is involved in smooth muscle-specific transcription. *J Cell Biol* 156: 983-991, 2002.

34. **Wang Z, Wang DZ, Hockemeyer D, McAnally J, Nordheim A, and Olson EN.** Myocardin and ternary complex factors compete for SRF to control smooth muscle gene expression. *Nature* 428: 185-189, 2004.

35. **Wilkins BJ, Dai YS, Bueno OF, Parsons SA, Xu J, Plank DM, Jones F, Kimball TR, and Molkentin JD.** Calcineurin/NFAT coupling participates in pathological, but not physiological, cardiac hypertrophy. *Circ Res* 94: 110-118, 2004.

36. **Viola JP, Carvalho LD, Fonseca BP, and Teixeira LK.** NFAT transcription factors: from cell cycle to tumor development. *Braz J Med Biol Res* 38: 335-344, 2005.

37. **Yellaturu CR, Ghosh SK, Rao RK, Jennings LK, Hassid A, and Rao GN.** A potential role for nuclear factor of activated T-cells in receptor tyrosine kinase and G-protein-coupled receptor agonist-induced cell proliferation. *Biochem J* 368: 183-190, 2002.

38. **Yu H, Sliedregt-Bol K, Overkleeft H, van der Marel GA, van Berkel TJC, and Biessen EAL.** Therapeutic Potential of a Synthetic Peptide Inhibitor of Nuclear Factor of Activated T Cells as Antirestenotic Agent 10.1161/01.ATV.0000225286.30710.af. *Arterioscler Thromb Vasc Biol* 26: 1531-1537, 2006.

39. **Zeidan A, Nordstrom I, Albinsson S, Malmqvist U, Sward K, and Hellstrand P.** Stretch-induced contractile differentiation of vascular smooth muscle: sensitivity to actin polymerization inhibitors. *Am J Physiol Cell Physiol* 284: C1387-1396, 2003.

40. **Zeidan A, Nordstrom I, Dreja K, Malmqvist U, and Hellstrand P.** Stretch-dependent modulation of contractility and growth in smooth muscle of rat portal vein. *Circ Res* 87: 228-234, 2000.

Figure legends

Figure 1. NFAT isoform expression. A. NFATc1, NFATc3 and NFATc4 are expressed in human myometrial arteries (*left panel*, n=6). No NFATc2 was detected (*right panel*), whereas amplification of the housekeeping gene HPRT is shown. **B.** Using the same primer pairs as in A, NFATc2 was detected in human Jurkat cells. **C.** NFAT isoform expression in cell explants from human myometrial arteries (hmVSMCs, n=2). **D.** NFATc2 expression after 4 day-culture of intact arteries (n=5). **E.** Western blotting for NFAT isoforms in myometrial arteries (indicated by arrows; n=2-4). *Asterisks:* 500 bp marker, *n*=patients.

Figure 2. Et-1 increases NFATc3 nuclear accumulation in VSMCs. A. Representative confocal images showing increased NFATc3 nuclear accumulation upon Et-1 treatment (10 nmol/L, 30 and 60 min) in hmVSMCs. Cells were pre-incubated in serum-free medium for 60 min before treatment. White indicates co-localization of NFATc3 (red) and the DNA binding dye SYTOX Green (green). Bars: 20 μm. **B.** Summarized time-course data from four experiments as in *A* (at least 40 cells were examined per time point and experiment, n=4). **C**. Representative confocal image of hmVSMCs stained for SM-α-actin (grey) and SYTOX Green (green). Bars: 20 μm. **D**. Western blot showing NFATc3 levels in nuclear fractions from control and Et-1 (50 nmol/L, 30 min) treated mVSMCs, in the presence or absence of A-285222 (upper panel). A-285222 (1.0 μmol/L) was present 30 min prior to and during Et-1 stimulation. The nuclear marker PCNA (bottom panel) was used for normalization. Experiments were performed twice and in duplicates.

Figure 3. A-285222 prevents Et-1-induced NFAT activation in native arteries. A. Representative confocal immunofluorescence images of NFATc3 nuclear accumulation in human

control arteries and after Et-1 treatment (10 nmol/L, 30 min at RT) with or without pre- and concurrent incubation with A-285222 (1 μmol/L). Co-localization of NFATc3 and SYTOX Green is shown in white. Bars: 20 μm. **B.** Percentage of NFATc3 nuclear accumulation in arteries, treated with Et-1 as in A, with or without A-285222 (0.1 and 1.0 μmol/L), CsA (1.0 μmol/L) or verapamil (1.0 μmol/L). 40-60 images from at least 12 arteries for each treatment were analyzed (n=4). **C**. The effect of Et-1 (50 nmol/L) with or without pre- and concurrent incubation with A-285222 or CsA (both 1.0 μmol/L) on NFAT-dependent luciferase activity is shown. Aortas from NFAT-luciferase transgenic mice were treated for 30 min and luciferase activity, expressed in relative luciferase units (RLU) per μg protein was measured after 6 hours (6 measurements for each condition, n=14). For comparison, background luciferase activity is shown in aortas from wild-type FVBN mice (n=2). ***$P < 0.001$, **$P < 0.01$, vs. control.

Figure 4. A-285222 reduces proliferation and cell number. A. HmVSMCs were incubated for 48 h in 0% FBS and 15% FBS (control) with or without A-285222 or CsA (both 1.0 μmol/L). PCNA fluorescence intensity in the nuclei normalized to control (3 experiments from n=3). **B.** Cell number after treatment as in A. Results are normalized to control (6 experiments from n=6). **C**. Summarized data from western blot analysis of cyclin D1 expression showing the effect of A-285222 (1.0 μmol/L) on Et-1-driven hmVSMCs proliferation (n=4 experiments). **D.** Dose-response for A-285222 and CsA effects on cell number evaluated as in B. Data was normalized to untreated control. ***$P < 0.001$, *$P < 0.05$ vs. control.

Figure 5. Down regulation of NFATc3 reduces VSMC proliferation. A. Representative confocal images showing NFATc3 expression (red) in hmVSMCs 72 h after transfection with non-targeting siCONTROL or NFATc3-specific siNFATc3 (82.5 nM). The right panel

shows summarized NFATc3 fluorescence intensity data, normalized to cell number as assessed by SYTOX Green fluorescence. Bars: 50 μm. **B.** Summarized data from western blot experiments showing NFATc3 and cyclin D1 expression in hmVSMCs 120 h after transfection with NFATc3-specific siNFATc3 (100 nM). Results are normalized to control (siCONTROL) and total protein in each sample assessed by Coomassie staining (n=5 experiments). Representative blots from the same gel showing down regulation of NFATc3 and cyclin D1 expression are shown above each graph.

Figure 6. Inhibition of NFAT reduces IL-6 production. Myometrial arteries were divided in pieces and cultured in parallel for 4 days in the presence or absence of A-285222 (0.1 or 1.0 μmol/L) or CsA (1.0 μmol/L). Media samples were collected at 24, 48, 72 and 96 hours, IL-6 concentration measured in duplicates and normalized to the protein content in the well. IL-6 concentration during culture (control, black squares) decreases in the presence of A-285222 (open triangles) or CsA (black circles). Results are normalized to control day 1 for each patient (n=4).

Figure 7. Chronic inhibition of NFAT has no effect on contractile protein synthesis. A. Representative Coomassie-stained gel showing vascular protein composition in myometrial arteries cultured for 4 days in the presence of 0.1 μmol/L A-285222 (lane 2), 1.0 μmol/L A-285222 (lane 3) or 1.0 μmol/L CsA (lane 4), compared to untreated control arteries (lane 1). Molecular weight standard is shown on the left. **B**. Summarized data from Coomassie-stained gels showing comparison of selected protein bands normalized to control (n=9). **C**. Autoradiograph with corresponding protein profile, showing [^{35}S]methionine incorporation during the last 24 h of the culture period (treatments and lane labels as in A). Asterisk indicates artifact due to crack in lane 4. **D**. Comparison of selected protein bands as well as

total protein synthesis from autoradiographs normalized to control and total protein content in each sample (n=2).

Figure 8. Chronic inhibition of NFAT has no effect on vascular contractility. Myometrial arteries were divided equal segments and cultured in parallel for 4 days in the presence (dashed lines) or absence (solid lines) of A-285222 (0.1 μmol/L) or CsA (1.0 μmol/L). **A and C**. Representative original force traces recorded after the 4 day-culture period, showing responses to HK (60 mmol/L) and Et-1 (10 nmol/L). Scale bars: 0.5 mN and 10 min. **B and D**. Summarized maximal wall tension upon HK or Et-1 stimulation from experiments as in A and C, expressed as recorded force divided by twice the vessel length, normalized to the number of cell layers (values from 8 arteries included in each bar, n=3 or n=2 for experiments using A-285222 or CsA, respectively).

Table 1: Primer pairs used in RT-PCR

	Forward	*Reverse*	*Fragment size*
NFATc1	5´-CTATCCTCTCCAACACCAAA-3´	5´-GTCAGTTTTCGCTTCCATCT-3´	416 bp
NFATc2	5´-GATGATGTAATGGACTATGGC-3´	5´-TAATGAGCAGGGATGTTTTG-3´	452 bp
NFATc3	5´-CTTTCAGTTCCTTCACCCTTTACC-3´	5´-TGCCAATATCAGTTTCTCCTTTTC-3´	499 bp
NFATc4	5´-CAGTCCTACCCAGAGTTTCAG-3´	5´-ACCTTATTGTATCCCTCAGCA-3´	504 bp
HPRT	5´- TTGCTGACCTGCTGGATTAC -3´	5´- CTGCATTGTTTTGCCAGTGT -3´	209 bp

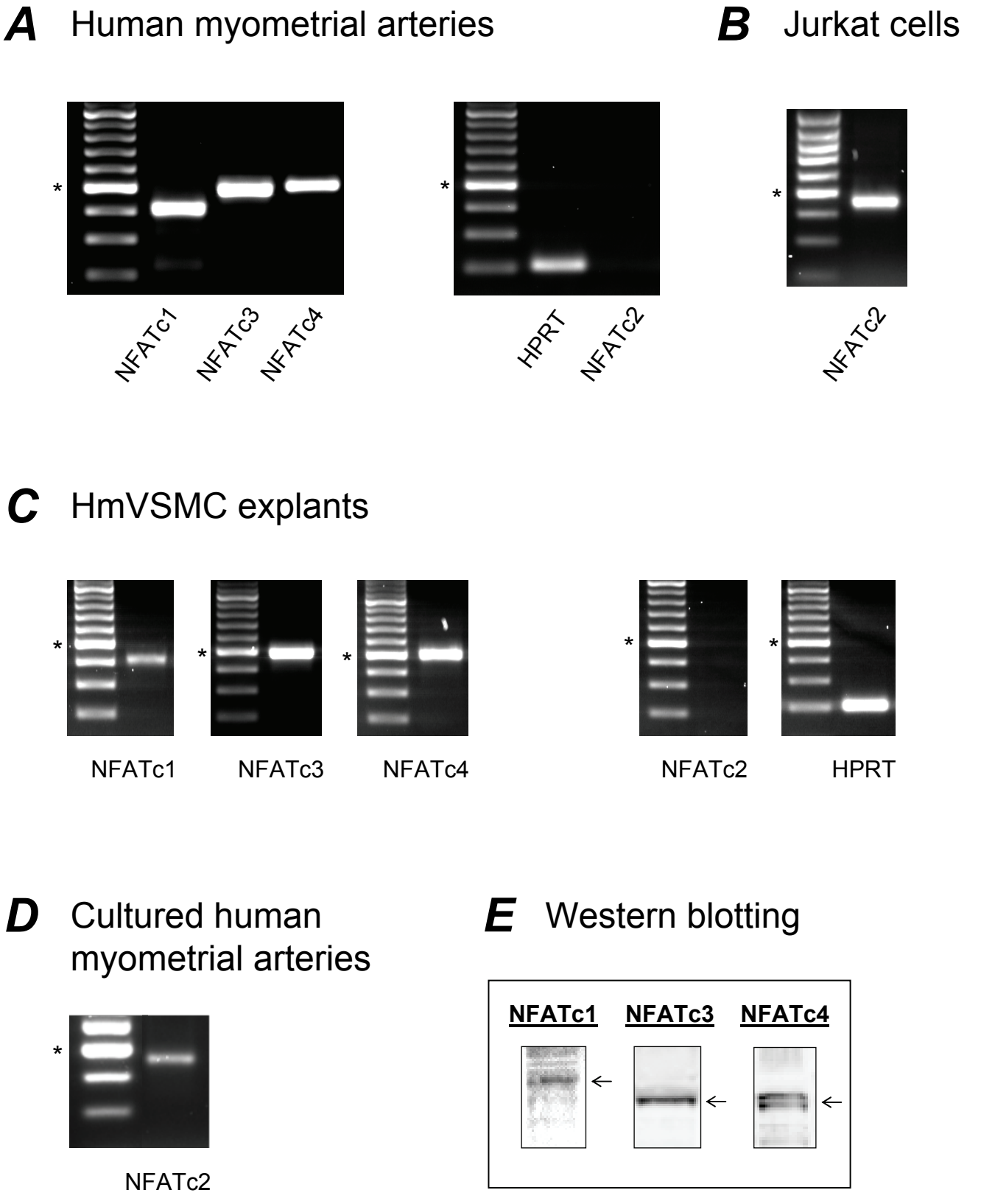
A Human myometrial arteries
B Jurkat cells
*
NFATc1
NFATc3
NFATc4
HPRT
NFATc2
C HmVSMC explants
NFATc1
NFATc3
NFATc4
NFATc2
HPRT
D Cultured human myometrial arteries
NFATc2
E Western blotting
NFATc1
NFATc3
NFATc4

Figure 1

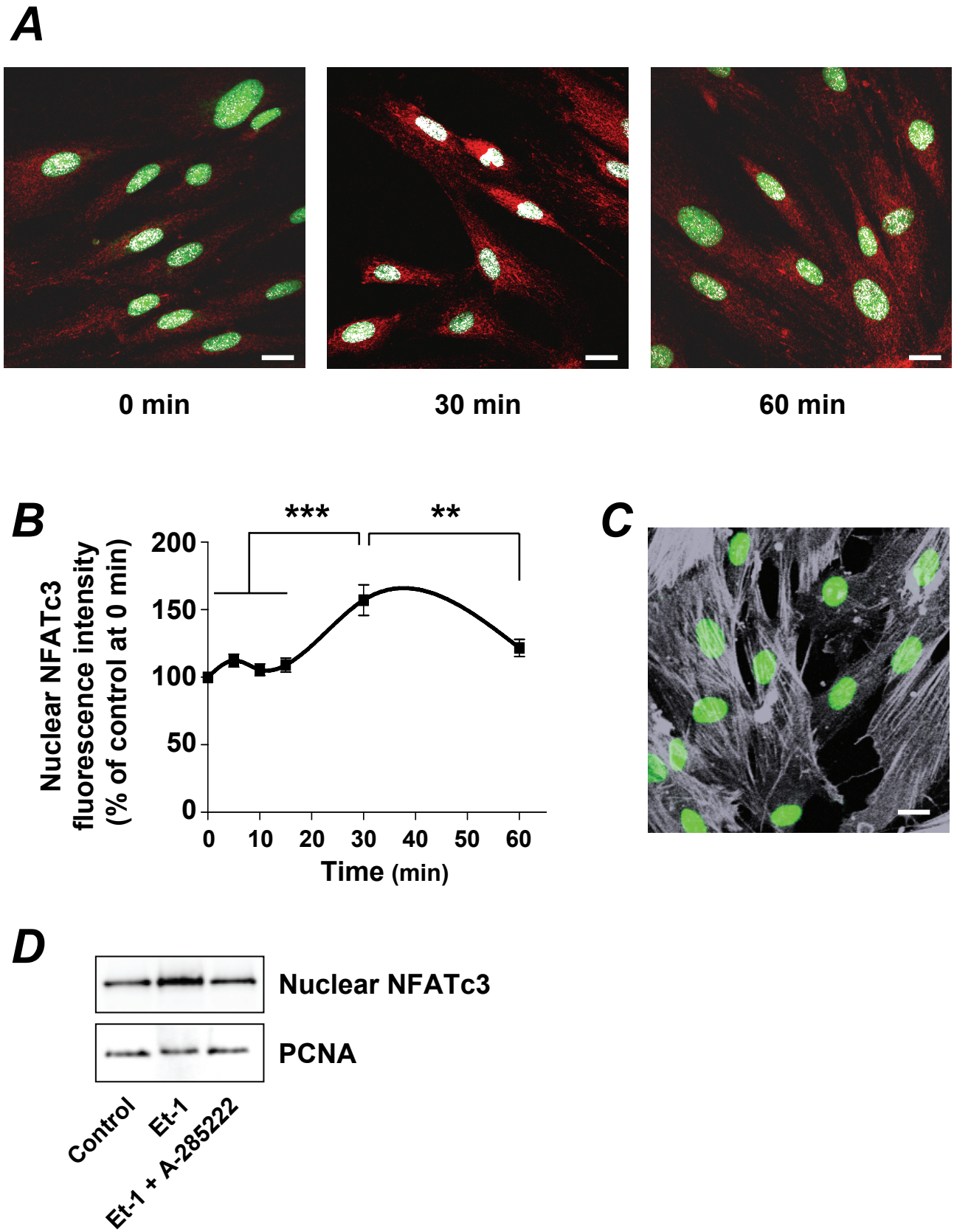
A
0 min
30 min
60 min
B
***
**
Nuclear NFATc3 fluorescence intensity (% of control at 0 min)
200
150
100
50
0
0
10
20
30
40
50
60
Time (min)
C
D
Nuclear NFATc3
PCNA
Control
Et-1
Et-1 + A-285222

Figure 2

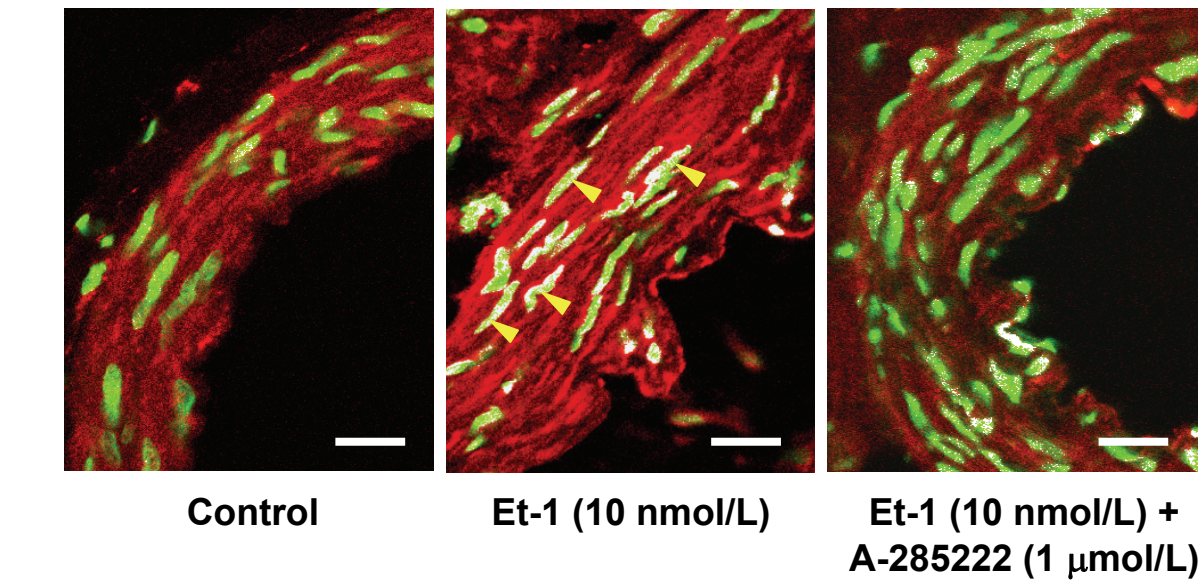
A
Control
Et-1 (10 nmol/L)
Et-1 (10 nmol/L) +
A-285222 (1 μmol/L)

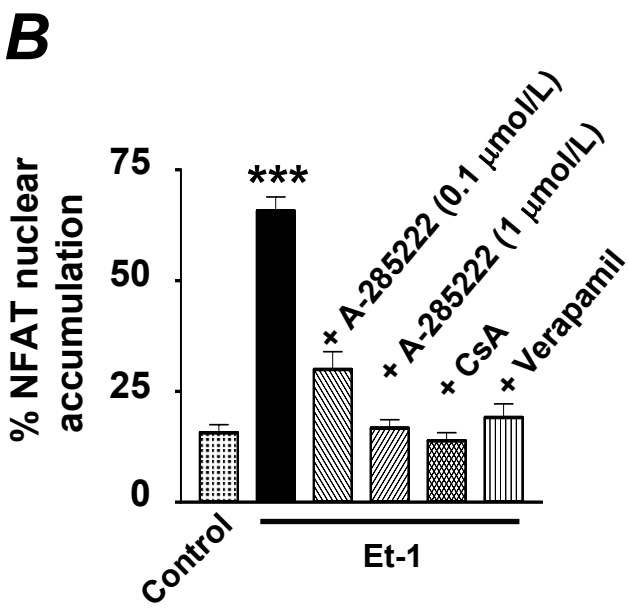
B
% NFAT nuclear accumulation
75
50
25
0
***
+ A-285222 (0.1 μmol/L)
+ A-285222 (1 μmol/L)
+ CsA
+ Verapamil
Control
Et-1

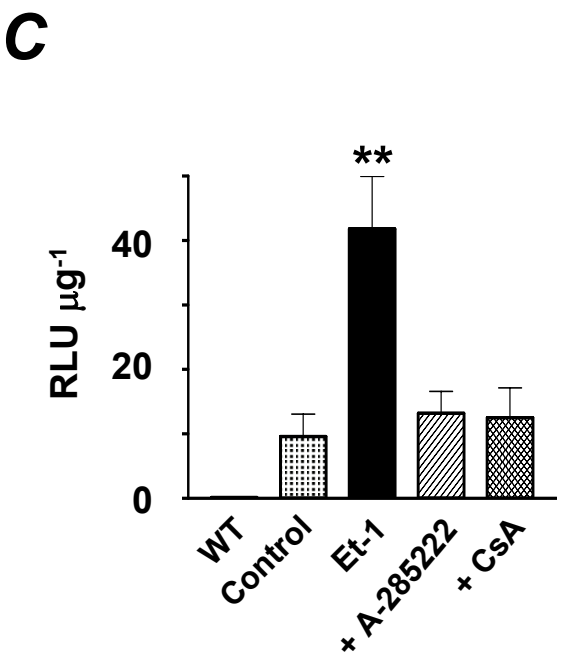
C
RLU μg-1
40
20
0
**
WT
Control
Et-1
+ A-285222
+ CsA

Figure 3

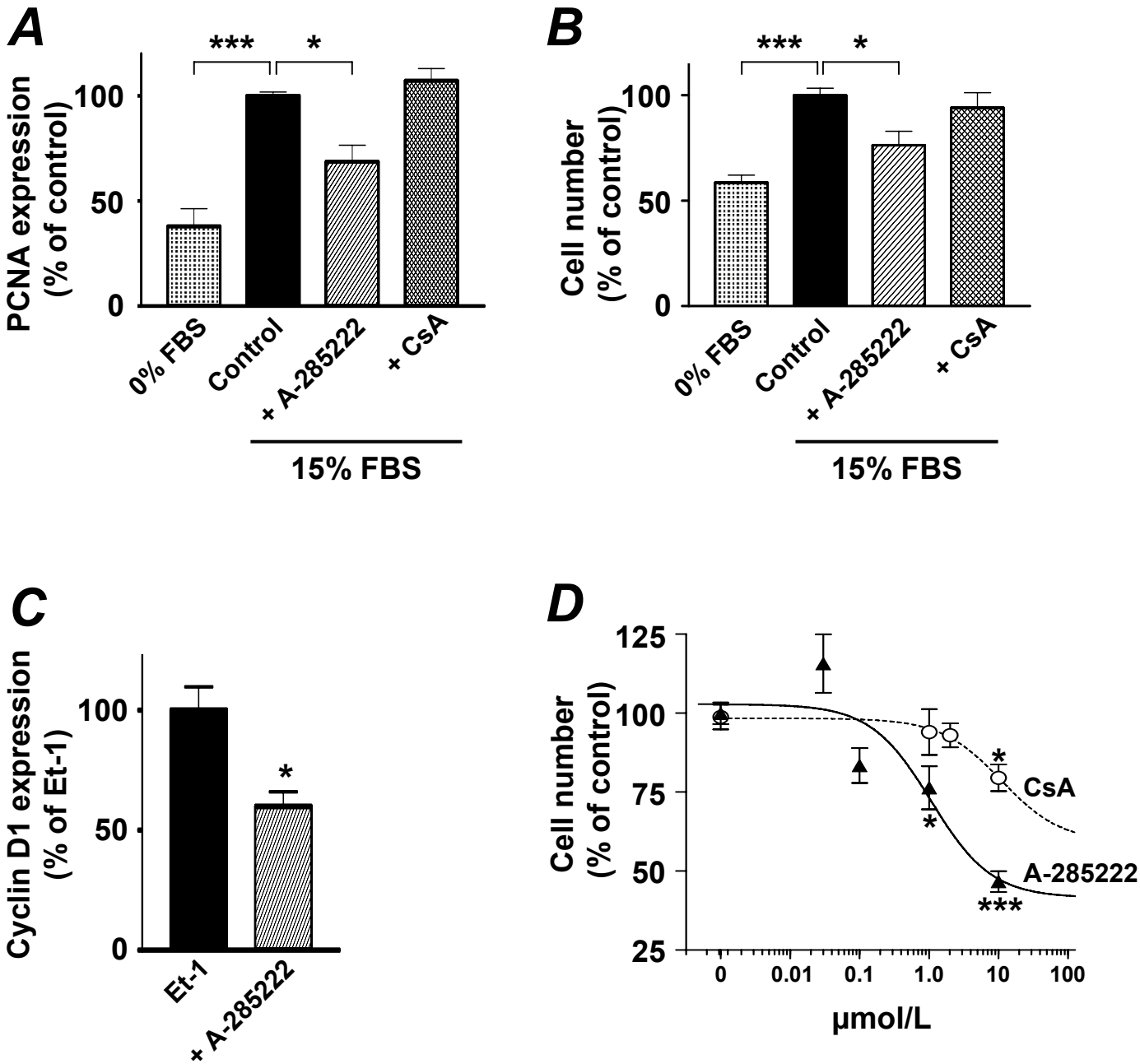
A
***
*
PCNA expression
(% of control)
100
50
0
0% FBS
Control
+ A-285222
+ CsA
15% FBS
B
***
*
Cell number
(% of control)
100
50
0
0% FBS
Control
+ A-285222
+ CsA
15% FBS
C
Cyclin D1 expression
(% of Et-1)
100
50
0
*
Et-1
+ A-285222
D
Cell number
(% of control)
125
100
75
50
25
*
*
***
CsA
A-285222
0
0.01
0.1
1.0
10
100
µmol/L

Figure 4

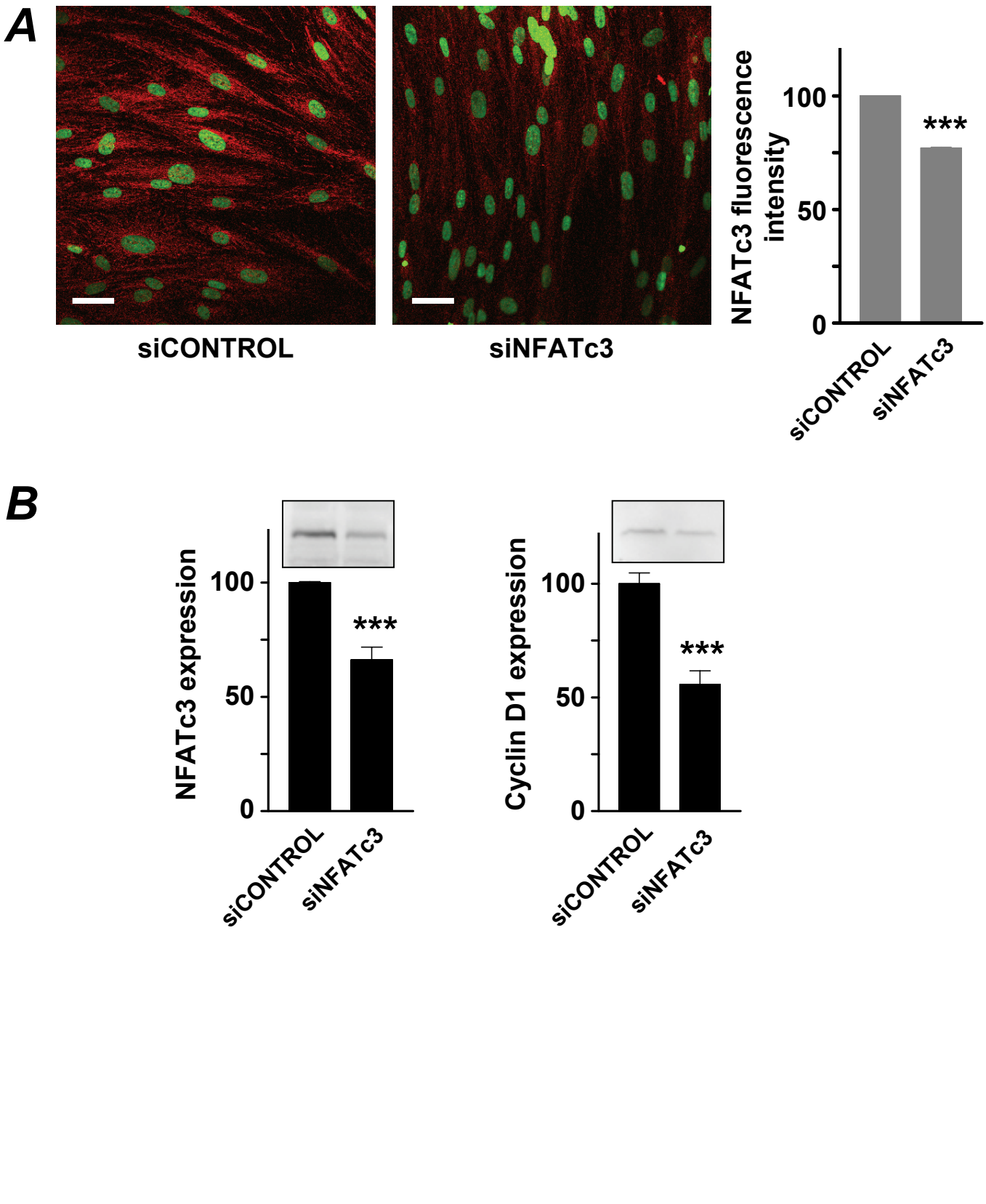
A
siCONTROL
siNFATc3
NFATc3 fluorescence intensity
100
50
0
***
siCONTROL
siNFATc3
B
NFATc3 expression
100
50
0
***
siCONTROL
siNFATc3
Cyclin D1 expression
100
50
0
***
siCONTROL
siNFATc3

Figure 5

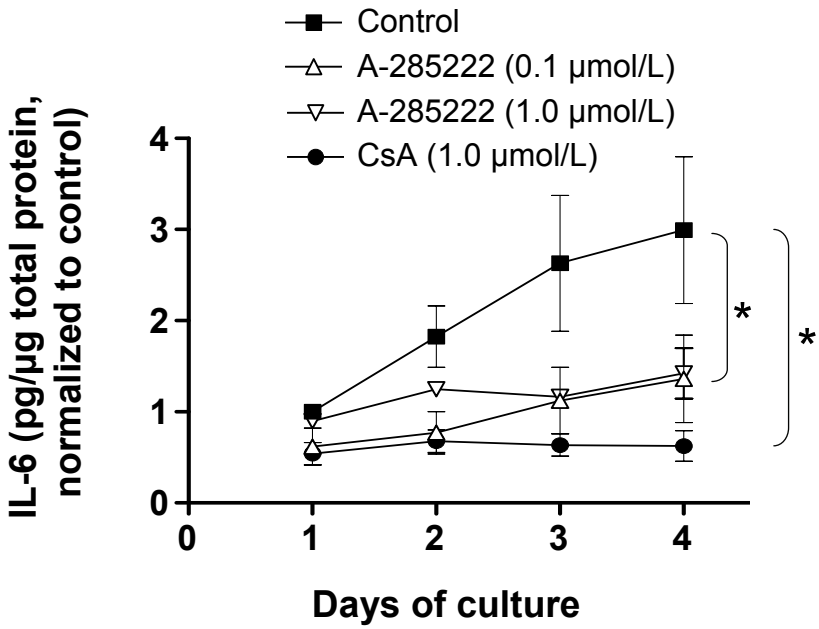
Control
A-285222 (0.1 µmol/L)
A-285222 (1.0 µmol/L)
CsA (1.0 µmol/L)
IL-6 (pg/µg total protein, normalized to control)
0
1
2
3
4
Days of culture
*
*

Figure 6

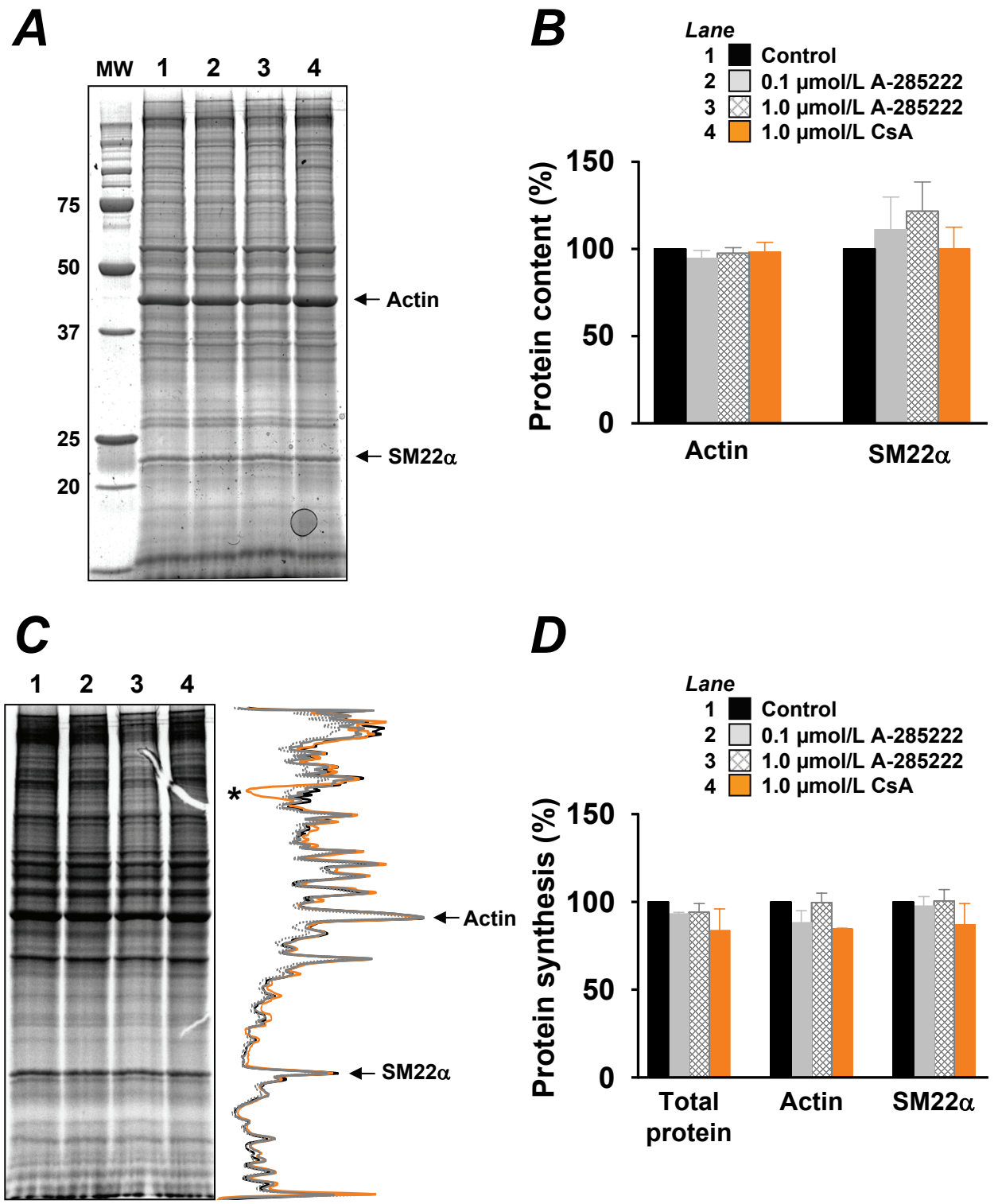
A
MW
1
2
3
4
75
50
37
25
20
Actin
SM22α
B
Lane
1 Control
2 0.1 μmol/L A-285222
3 1.0 μmol/L A-285222
4 1.0 μmol/L CsA
Protein content (%)
150
100
50
0
Actin
SM22α
C
1
2
3
4
*
Actin
SM22α
D
Lane
1 Control
2 0.1 μmol/L A-285222
3 1.0 μmol/L A-285222
4 1.0 μmol/L CsA
Protein synthesis (%)
150
100
50
0
Total protein
Actin
SM22α

Figure 7

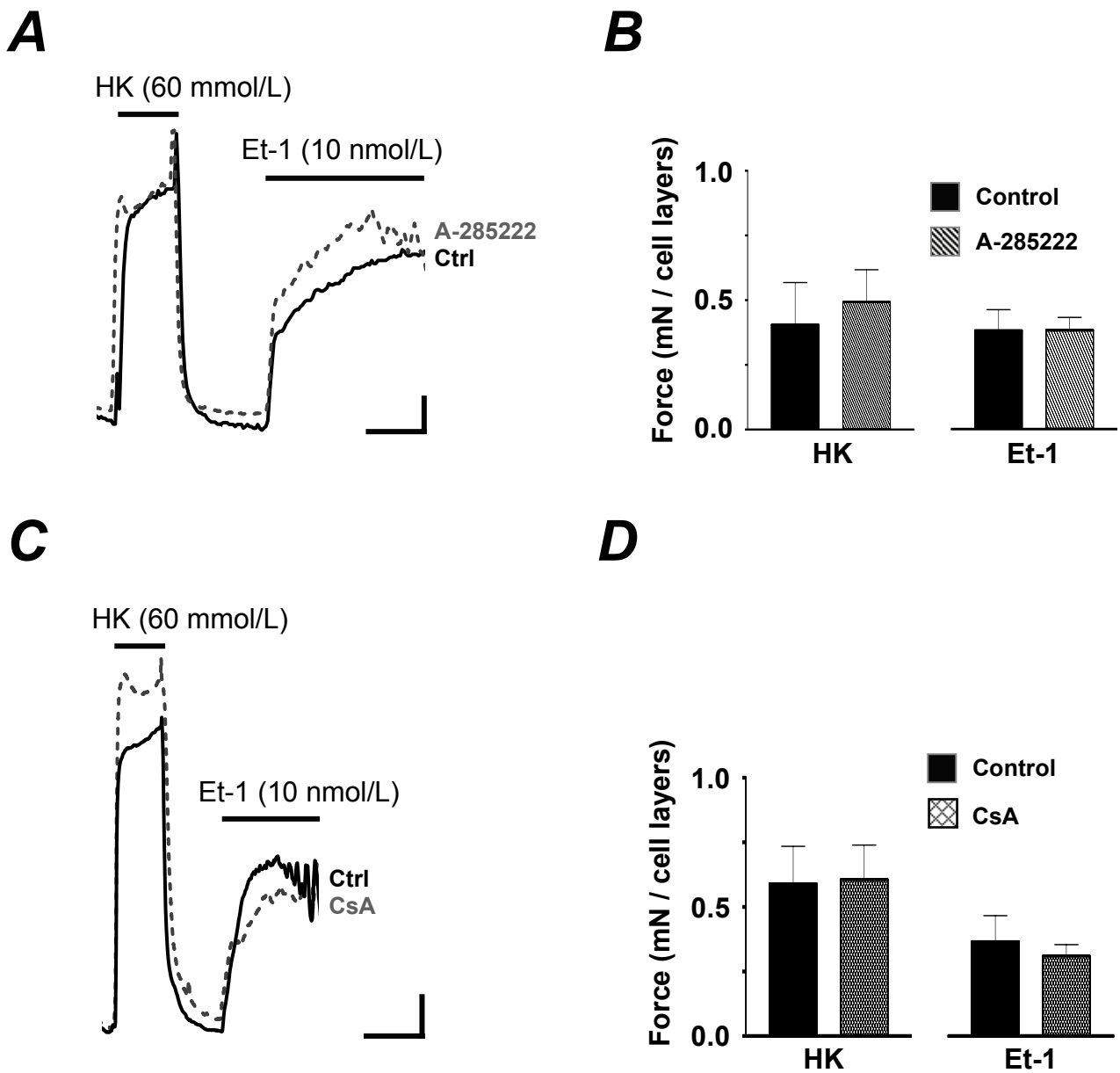
A
HK (60 mmol/L)
Et-1 (10 nmol/L)
A-285222
Ctrl
B
Force (mN / cell layers)
1.0
0.5
0.0
Control
A-285222
HK
Et-1
C
HK (60 mmol/L)
Et-1 (10 nmol/L)
Ctrl
CsA
D
Force (mN / cell layers)
1.0
0.5
0.0
Control
CsA
HK
Et-1

Figure 8